CHALMERS
UNIVERSITY OF TECHNOLOGY

1060 nm VCSELs for long-reach optical interconnects

Optical Fiber Technology 44 (2018) 36–42

Contents lists available at ScienceDirect

Optical Fiber Technology

journal homepage: www.elsevier.com/locate/yofte

Regular Articles

1060 nm VCSELs for long-reach optical interconnects

A. Larsson[a,*], E. Simpanen[a], J.S. Gustavsson[a], E. Haglund[a], E.P. Haglund[a], T. Lengyel[a], P.A. Andrekson[a], W.V. Sorin[b], S. Mathai[b], M. Tan[b], S.R. Bickham[c]

[a] Photonics Laboratory, Department of Microtechnology and Nanoscience, Chalmers University of Technology, SE-41296 Göteborg, Sweden
[b] Hewlett Packard Enterprise, 1501 Page Mill Road, Palo Alto, CA 94304-1123, USA
[c] Corning Research and Development Corporation, 1 Science Center Drive, Painted Post, NY 14870, USA

ARTICLE INFO

Keywords:
Vertical-cavity surface-emitting laser
Multimode fiber
Optical interconnects
Long-reach
1060 nm

ABSTRACT

Reach extension of high capacity optical interconnects based on vertical-cavity surface-emitting lasers (VCSELs) and multimode fibers (MMFs), as needed for large-scale data centers, would benefit from high-speed GaAs-based VCSELs at 1060 nm. At this wavelength, the chromatic dispersion and attenuation of the optical fiber are much reduced in comparison with 850 nm. We present single and multimode 1060 nm VCSELs based on designs derived partly from our high-speed 850 nm VCSEL designs. The single-mode VCSEL, with a modulation bandwidth exceeding 22 GHz, supports back-to-back data rates up to 50 Gbps at 25 °C and 40 Gbps at 85 °C under binary NRZ (OOK) modulation. Using mode-selective launch, we demonstrate error-free 25 Gbps transmission over 1000 m of 1060 nm optimized MMF. Higher data rates and/or longer distances will be possible with equalization, forward-error-correction, and/or multilevel modulation.

1. Introduction

The short-reach optical interconnects used in data centers are dominated by 850 nm vertical-cavity surface-emitting laser (VCSEL) and multimode fiber (MMF) links with reach up to ~100 m at high data rates (i.e. 25–28 Gbps OOK and 50–56 Gbps PAM-4) when employing OM4 MMF [1,2]. The VCSEL-MMF technology is the most cost-efficient due to low VCSEL manufacturing and packaging costs enabled by wafer-scale testing and screening, the self-hermeticity of the VCSEL, the large alignment tolerance to the MMF, and the use of plastic coupling optics. VCSELs also offer the high energy efficiency and small footprint needed for low power consumption and high bandwidth density.

With data centers growing in size, there is a need for optical interconnects with a reach beyond 1 km. At 850 nm, the fiber chromatic dispersion is as high as −85 ps/nm/km [3]. Therefore, the reach of 850 nm VCSEL-MMF links with *multimode* VCSELs and high modal bandwidth OM4 fiber is limited by chromatic dispersion at high data rates. It has been shown that the impact of chromatic dispersion can be mitigated using MMF exhibiting modal-chromatic dispersion compensation properties or *single-mode* VCSELs with a narrow spectral width. The former has enabled 56 Gbps PAM-4 over 200 m OM4 fiber using equalization and forward-error-correction (FEC) [4]. The latter has enabled, for instance, 25 Gbps OOK over 1300 m OM4 fiber without equalization or FEC [5], 54 Gbps OOK over 2200 m OM4 fiber with equalization and FEC [6], 49 Gbps transmission over 2200 m OM4 fiber using DMT modulation and FEC [7], and 135 Gbps DMT over 550 m OM4 fiber with equalization and FEC [8]. Single-mode VCSELs reduce not only the impact of chromatic dispersion but also the impact of modal dispersion through selective launch into specific modes groups of the MMF, but at the cost of a higher required alignment precision. More limited reach extension at high data rates has been demonstrated with multimode VCSELs by improving VCSEL parameters such as modulation bandwidth, rise and fall times, and intensity noise, and using techniques such as pre-emphasis, equalization, and advanced modulation formats. This includes 60 Gbps OOK over 107 m OM3 fiber using equalization (no FEC) [9], 64 Gbps PAM-4 over 2000 m OM4 fiber using equalization and FEC [10], and 100 (70) Gbps duobinary PAM-4 over 300 (500) m OM4 fiber with equalization and FEC [11]. In addition, shortwave wavelength division multiplexing with 4 channels (SWDM4) has demonstrated 212 Gbps (4 × 53 Gbps PAM-4) and 400 Gbps (4 × 100 Gbps PAM-4) over 300 and 105 m of wideband-MMF, respectively, both using equalization and FEC [12,13], and 176 Gbps (4 × 44 Gbps OOK) over 100 m OM4 fiber using equalization but no FEC [14]. In many of these links, heavy use of FEC and other forms of digital signal processing (DSP) is needed to mitigate impairments caused by the limited bandwidth and nonlinear response of the VCSEL, and the fiber modal and chromatic dispersion. This leads to increased complexity, latency, and power consumption. In addition, at 850 nm, fiber attenuation exceeds 2 dB/km [3], which is demanding for the power budget when attempting to increase the reach beyond 1 km at

* Corresponding author.
E-mail address: anders.larsson@chalmers.se (A. Larsson).

https://doi.org/10.1016/j.yofte.2018.01.001
Received 3 May 2017; Received in revised form 6 November 2017; Accepted 3 January 2018
Available online 08 January 2018

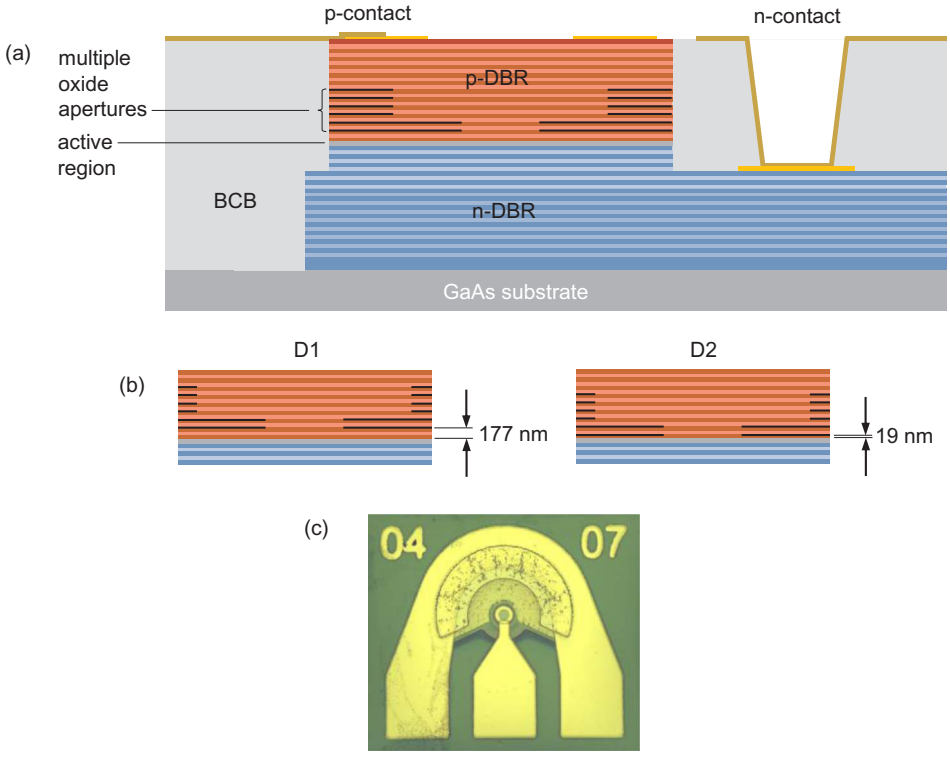

Fig. 1. (a) Cross-sectional view to illustrate the multiple oxide apertures (2 primary and 4 secondary) used for confinement and capacitance reduction. (b) Positioning of oxide apertures relative the active region for designs D1 and D2. (c) Microscope top image showing the emission aperture and the ground-signal-ground contact pads.

Table 1
Summary of basic static and dynamic performance parameters at low (25 °C) and high (85 °C) temperature.

Design	**D1**		**D2**	
Aperture diameter (μm)	**7**		**4**	
Temperature (°C)	25	85	25	85
Threshold current (mA)	0.65	1.06	0.19	0.34
Slope efficiency (W/A)	0.48	0.41	0.44	0.36
Differential resistance (Ω)	80	90	250	270
Modulation bandwidth (GHz)	19.9	15.0	22.3	15.6
D (GHz/mA$^{1/2}$)	8.2	6.4	17.6	13.7
K (ns)	0.22	0.29	0.16	0.22
f_p (GHz)	12.5	11.5	11.5	8.8

high data rates, especially for lower power single-mode VCSELs.

Clearly, extending reach would benefit from improved fiber performance to enable system implementations with simple modulation formats and a minimum of DSP. The fiber performance in terms of chromatic dispersion and attenuation improves at longer wavelengths [3]. The ideal wavelength is 1310 nm where chromatic dispersion is near zero and attenuation of MMF is only ~0.4 dB/km. However, the GaAs-based VCSEL technology, which is superior to the InP-based in terms of speed, efficiency, manufacturability, and cost-efficiency, can only be extended to ~1100 nm using conventional compound semiconductors without compromising reliability [15]. This has created an interest in GaAs-based VCSELs at wavelengths just below 1100 nm where the fiber chromatic dispersion is −30 ps/nm/km and attenuation is below 1 dB/km [3]. These are large improvements with respect to 850 nm. For MMF, the refractive index profile must also be optimized to minimize the differential mode delay for high modal bandwidth at the operating wavelength. For instance, when moving from 850 to 1060 nm, the alpha-value of the graded index MMF has to be reduced from ~2.10 to ~2.06 [3].

The first reports on near 1100 nm VCSELs came from NEC. Using strained InGaAs/GaAs quantum wells (QWs) with doped barriers for high differential gain and reduced gain compression, and implantation to reduce capacitance, oxide-confined multimode VCSELs at 1090 nm with a modulation bandwidth of 20 GHz and transmission capacity of 25 Gbps OOK were demonstrated in 2006 [16]. With strained InGaAs/GaAsP QWs, the high temperature performance was improved and 25 Gbps OOK data transmission at 100 °C was demonstrated [15]. The oxide aperture was also replaced by a buried-tunnel junction, which allows for current injection through an intra-cavity n-GaAs layer for low resistance [17]. With a bandwidth of 24 GHz, this VCSEL enabled data transmission at 40 Gbps OOK [18]. Work on 1060 nm VCSELs has been conducted at UC Santa Barbara. Using strained InGaAs/GaAs QWs with doped barriers and multiple oxide apertures for low capacitance, bottom-emitting VCSELs with a bandwidth of 18 GHz and operation at 25 Gbps OOK [19] were demonstrated. The data rate was extended to 30 Gbps using pre-emphasis and FEC [20]. However, most of the work on 1060 nm VCSELs has been conducted by Furukawa [21]. Using double intra-cavity contacts and a dielectric top distributed Bragg reflector (DBR), low-resistance high-efficiency oxide-confined VCSELs with a modulation bandwidth of 20 GHz were demonstrated. This enabled transmission at 25 and 28 Gbps OOK over 1000 and 500 m of 1060 nm optimized MMF, respectively [22–24]. With VCSELs from Furukawa, Georgia Tech demonstrated 50 Gbps PAM-4 transmission over 310 m of wideband MMF using pre-emphasis and FEC [25]. Finally, Hewlett Packard Labs have demonstrated 990–1065 nm oxide-confined, bottom emitting, and lens-integrated VCSELs with strain-compensated InGaAs/GaAsP QWs and transmission at 25 Gbps OOK over 75 m of OM3 fiber [26]. They also recently demonstrated 25 Gbps OOK and 50 Gbps PAM-4 transmission over 2000 m of standard single-mode fiber using a single-mode version of the 1065 nm VCSEL [27].

At the somewhat shorter wavelength of 980 nm, where the improvements of fiber chromatic dispersion and attenuation are not as large, very small aperture oxide-confined VCSELs with a modulation bandwidth exceeding 30 GHz were demonstrated recently [28]. With a larger aperture size, data transmission at 50 Gbps up to 75 °C was achieved [29].

In the following, we present the design and performance of our recently developed 1060 nm VCSELs, as well as results from preliminary data transmission experiments using a prototype 1060 nm

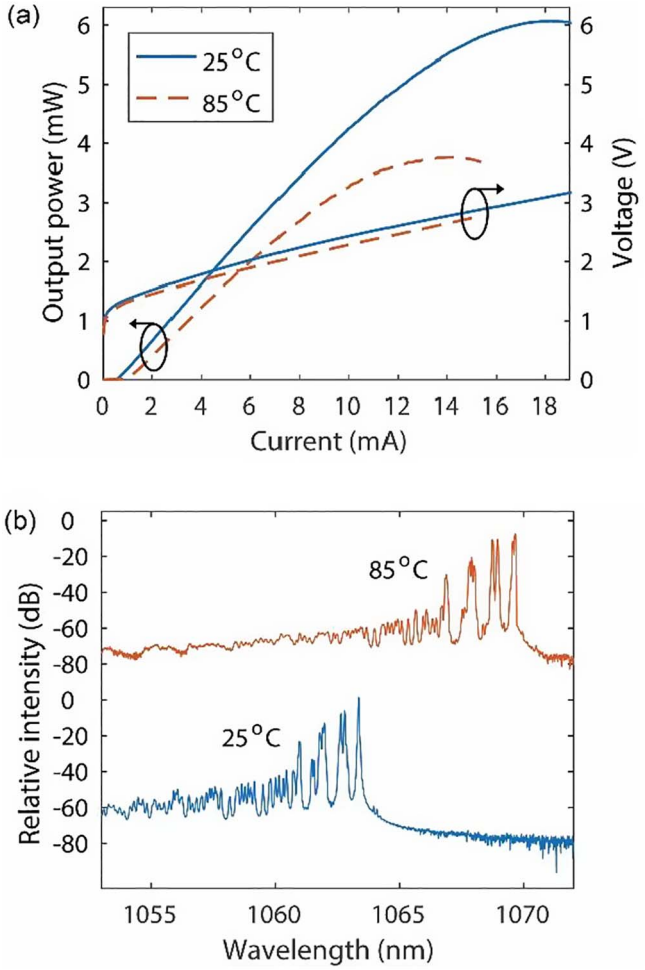

Fig. 2. Steady-state characteristics for a D1-VCSEL with a 7 μm oxide aperture at 25 and 85 °C. (a) Output power and voltage vs. current. (b) Emission spectra.

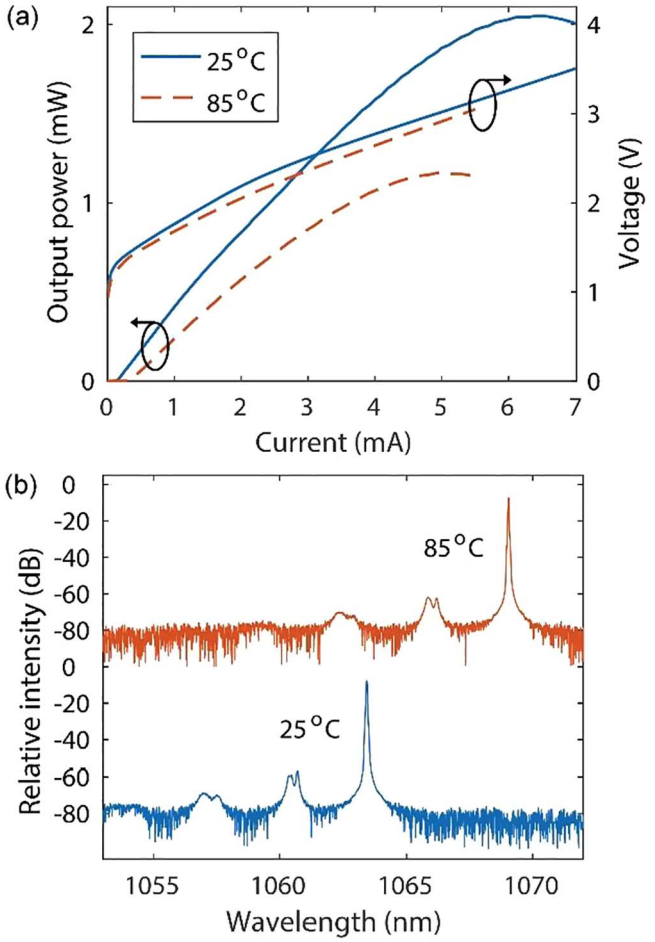

Fig. 3. Steady-state characteristics for a D2-VCSEL with a 4 μm oxide aperture at 25 and 85 °C. (a) Output power and voltage vs. current. (b) Emission spectra.

optimized MMF designed and manufactured by Corning. The VCSEL designs and fabrication are presented in Section 2 and their basic static and dynamic performance characteristics are presented in Section 3. Section 4 is devoted to the data transmission experiments and a summary and outlook is presented in Section 5.

2. VCSEL design and fabrication

The GaAs-based 1060 nm VCSEL designs are derived from our previous all-semiconductor 850 nm designs, which have enabled up to 30 GHz modulation bandwidth [30,31]. Two designs, referred to as D1 and D2, have been developed. They have the following in common with the 850 nm designs. For high longitudinal optical confinement, we use a short half-wavelength-thick cavity. For low resistance and low internal optical loss, we use modulation doping and graded composition interfaces in the DBRs. Parabolic interface grading is used in the top p-DBR while step-grading is used in the bottom n-DBR. In both DBRs, the average doping level is reduced towards the center of the cavity to minimize loss due to free-carrier absorption and minimize the resistance-loss product [32]. The first 24 pairs in the bottom DBR are made of AlAs/GaAs to reduce the thermal impedance. All other mirror pairs are made of $Al_{0.9}Ga_{0.1}As$/GaAs. Multiple oxide apertures are placed in the p-DBR just above the active region (Fig. 1). The two primary oxide apertures provide transverse optical and current confinement, while the four secondary reduce the capacitance associated with charge stored over the oxide layers.

With respect to the 850 nm VCSEL designs, a number of modifications were implemented. In the active region, we use three partially strain-compensated InGaAs/GaAsP quantum wells (QWs), with net compressive strain, rather than the five InGaAs/GaAs QWs used in the 850 nm designs. In design D1, both the $Al_{0.98}Ga_{0.02}As$ primary and the $Al_{0.96}Ga_{0.04}As$ secondary oxide layers are 30 nm thick, as in the 850 nm designs. However, the Al-content in the AlGaAs layers neighboring the primary oxide layers is reduced to reduce the rate of vertical oxidation into these layers to form oxide apertures with long tapers [33]. This, together with positioning the primary oxide apertures at optical field nodes, reduces the strength of the transverse index guiding. In design D2, we also reduced the thickness of the primary oxide layers to 20 nm to further reduce guiding. The cold-cavity effective index difference between the oxidized and non-oxidized parts of the cavity, calculated using an effective index model [34], is 0.00165 for D1 and only 0.000654 for D2. The weak guiding is used to reduce the number of active transverse modes, thereby reducing the spectral width and beam divergence. It also enables the fabrication of single-mode VCSELs with relatively large oxide apertures. A drawback of the thinner oxide layers is an increased oxide capacitance. Finally, designs D1 and D2 differ in the positioning of the first primary oxide aperture with respect to the active region (Fig. 1). In D1, it is at a relatively large distance of 177 nm from the active region while in D2 it is much closer, at a distance of only 19 nm. This suppresses transverse current spreading which improves the transverse confinement of carriers and optical gain. This leads to the gain being more mode selective, which favors the fundamental LP_{01} mode.

A general difference between VCSELs at 850 and 1060 nm is the higher internal optical loss at longer wavelengths due to the quadratic

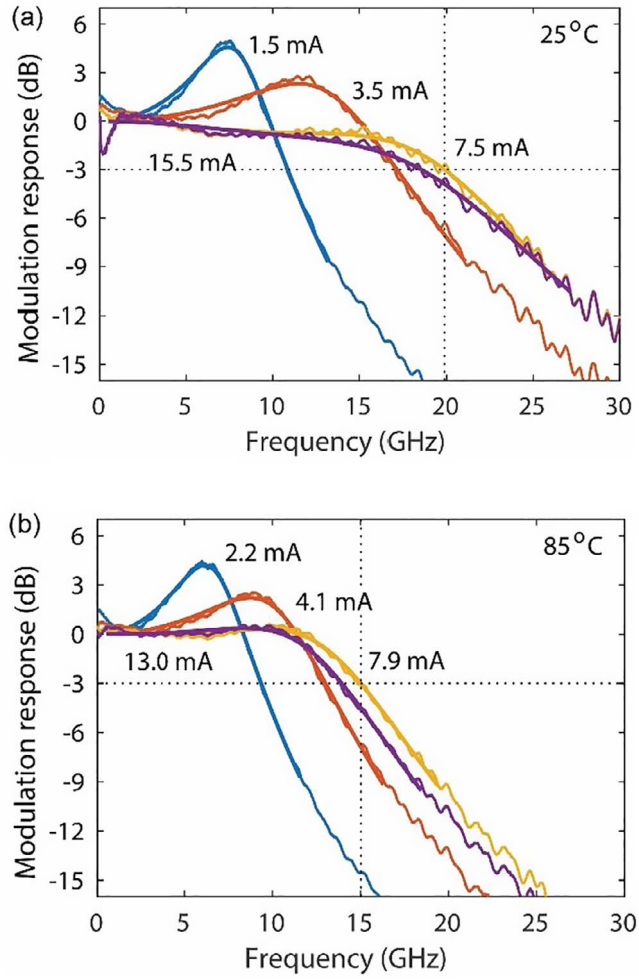

Fig. 4. Small signal modulation response at different bias currents for the multimode D1-VCSEL (7 μm oxide aperture) at (a) 25 °C and (b) 85 °C.

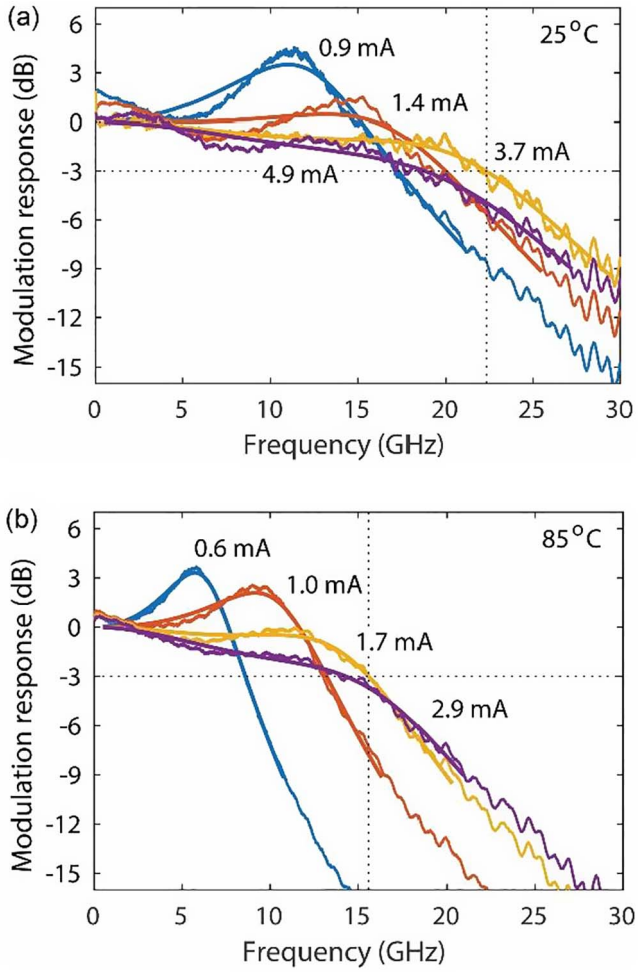

Fig. 5. Small signal modulation response at different bias currents for the single-mode D2-VCSEL (4 μm oxide aperture) at (a) 25 °C and (b) 85 °C.

dependence of free-carrier absorption on wavelength [35]. With similar designs, VCSELs at 1060 nm therefore have lower slope efficiency and power efficiency. Since absorption generates heat, it also reduces the thermal rollover current and the maximum output power.

The epitaxial structures were grown by metal-organic chemical vapor deposition on an undoped GaAs substrate. Standard fabrication techniques were used for mesa etching, deposition and etching of dielectrics, deposition of contact and pad metals, and selective oxidation. A thick layer of benzocyclobutene (BCB) was used under the p-bondpad to reduce the pad capacitance. The diameter of the top mesa was varied from 15 to 21 μm to have VCSELs with different oxide aperture diameter from a single oxidation. Since the thickness of the topmost layer of the top DBR has a large impact on the cavity photon lifetime and therefore the VCSEL dynamics, it was carefully adjusted by dry etching for a damped high-bandwidth modulation response [36]. A microscope image of a fabricated VCSEL is shown in Fig. 1.

3. VCSEL performance

For both designs, VCSELs with an aperture size in the range 3–7 μm were characterized. D2 is particularly useful for the fabrication of single-mode VCSELs as it has the weakest transverse guiding and the most strongly confined gain. In the following, we therefore present results from measurements on one VCSEL from design D1: a 7 μm aperture multimode VCSEL, and one VCSEL from design D2: a 4 μm aperture single-mode VCSEL. For convenience, basic static and dynamic performance parameters at 25 and 85 °C are summarized in Table 1.

For all VCSELs, the thickness of the topmost layer of the top DBR was adjusted to set the cavity photon lifetime to ~4 ps at room temperature. This should yield a high-bandwidth critically damped modulation response to suppress overshoot and ringing under large signal modulation and reduce inter-symbol interference when transmitting data [37]. From calculations of DBR transmission losses using a transfer matrix model and the internal optical loss using the effective index model, we estimate a slope efficiency of ~0.45 W/A at 4 ps photon lifetime and used this as a target performance parameters when adjusting the thickness of the top layer.

3.1. Steady-state characteristics

The measured output power and voltage vs. current and emission spectra are shown in Figs. 2 and 3. When comparing VCSELs with the same aperture size, the threshold currents for VCSELs from design D2 were consistently lower due to the stronger transverse current confinement and therefore less transverse current spreading and leakage. The VCSELs have a room temperature slope efficiency close to the target value of 0.45 W/A. The differential resistance, measured at half the rollover current, is similar to that of our 850 nm VCSELs and scales rapidly with aperture size for small apertures.

The emission spectra show that the 4 μm D2-VCSEL is strongly single-mode with > 50 dB suppression of higher order modes at all currents and temperatures. This is due to the weak guiding and strong confinement which enables single-mode operation with a relatively large aperture and therefore low resistance (~250 Ω).

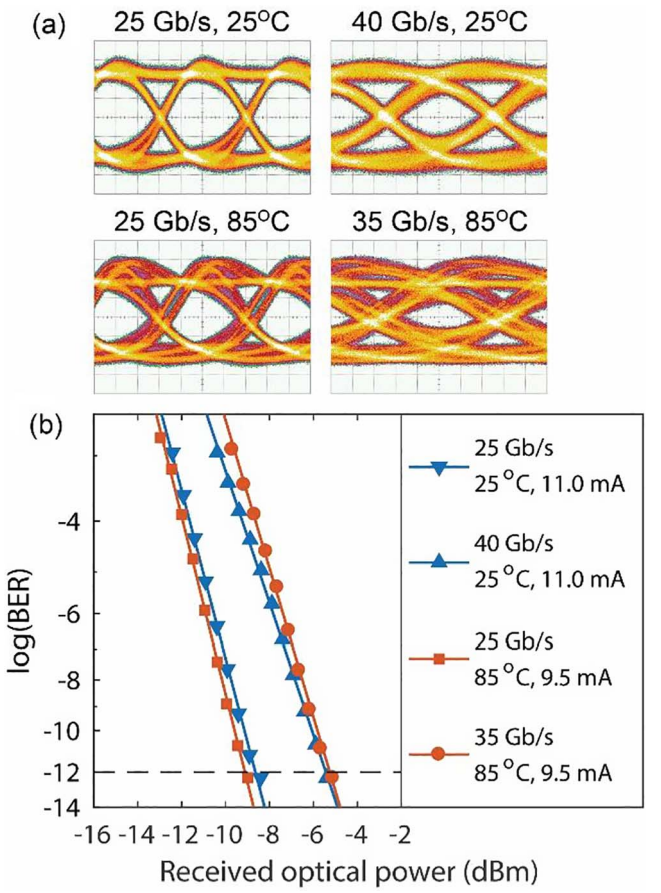

Fig. 6. Large signal modulation response for the multimode D1-VCSEL (7 μm oxide aperture) under OOK NRZ modulation at different bit rates and temperatures. (a) Eye diagrams of the received signals. (b) BER vs. received optical power. The modulation voltage is 800 mV. Bias currents are 11 mA at 25 °C and 9.5 mA at 85 °C.

3.2. Small-signal modulation

The small-signal modulation response ($|S_{21}|$) was measured using a 28 GHz photodetector (Picometrix DG32-xr) and a 67 GHz vector network analyzer (Rohde & Schwartz ZVA) with the light from the VCSEL coupled to a short OM4 fiber. The results are shown in Figs. 4 and 5. At room temperature, the smaller size single-mode (D2) VCSEL reaches a bandwidth of 22 GHz while the larger size multimode (D1) VCSEL has a slightly lower bandwidth. At 85 °C, the modulation bandwidths are reduced by a few GHz. Both VCSELs reach maximum bandwidth at a bias current approximately half the rollover current. At this current, the modulation response is damped and relatively flat.

The conventional three-pole transfer function was fitted to the measured modulation response to extract *D*- and *K*-factors and the parasitic pole frequencies (f_p) [31]. Numbers are listed in Table 1. Compared to the 850 nm VCSELs, the 1060 nm VCSELs have a few GHz lower bandwidth, which is due to the use of thinner oxide layers with higher capacitance. This conclusion is supported by the extracted parasitic pole frequencies being a few GHz lower.

3.3. Large-signal modulation

The large-signal modulation response was assessed by back-to-back OOK data transmission over a short OM4 fiber. Data (NRZ PRBS-7 with 800–1000 mV peak-to-peak amplitude) was generated using a pattern generator (SHF 12103A) and a 55 GHz amplifier (SHF 804 TL) to drive the VCSEL. After a variable optical attenuator, the optical signal was detected by a 30 GHz linear optical receiver (Picometrix PT-28B) and analyzed using an error analyzer (SHF 1110B) to determine the bit-error-ratio (BER). Eye diagrams of the received signals were recorded using a 70 GHz equivalent time sampling oscilloscope (Agilent 86100C). The results are shown in Figs. 6 and 7.

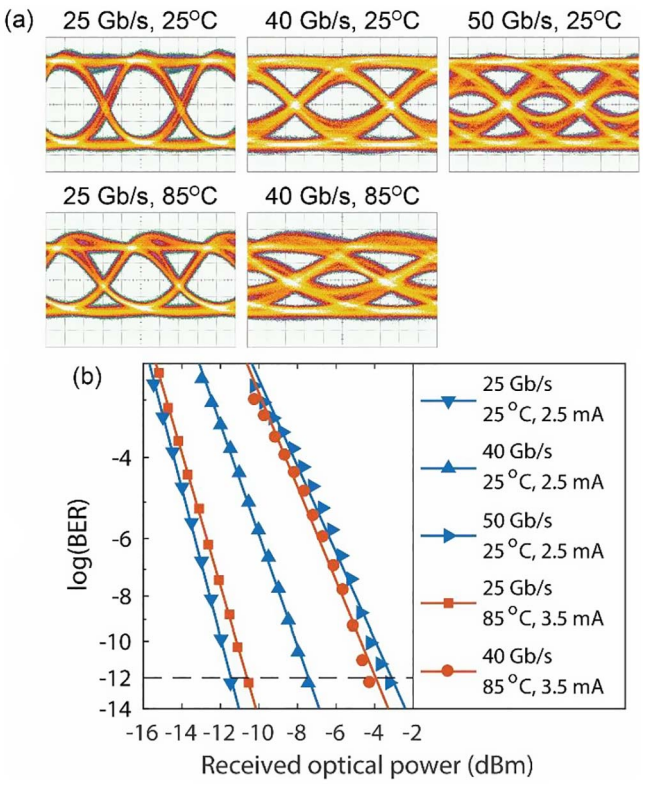

Fig. 7. Large signal modulation response for a single-mode D2-VCSEL (4 μm oxide aperture) under OOK NRZ modulation at different bit rates and temperatures. (a) Eye diagrams of the received signals. (b) BER vs. received optical power. The modulation voltage is 1000 mV. Bias currents are 2.5 mA at 25 °C and 3.5 mA at 85 °C.

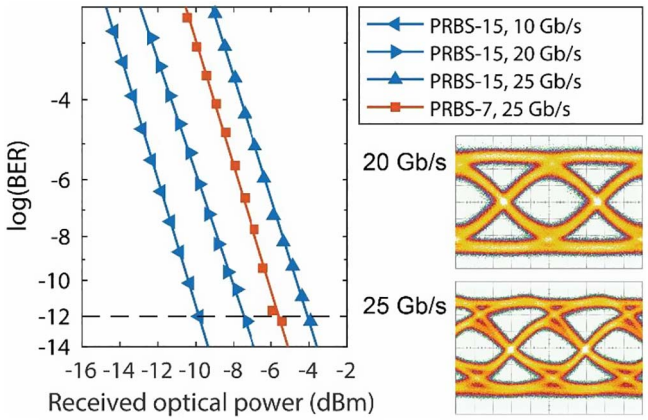

Fig. 8. Results from data transmission over 1000 m of 1060 nm optimized MMF, showing BER vs. received optical power for bit-rates of 10, 20, and 25 Gbps at PRBS-15 (25 Gbps is also shown at PRBS-7). Eye-diagrams are shown to the right.

At room temperature, both VCSELs show the response of a close to critically damped system, as revealed by the linear optical receiver. At the higher temperature, there is a tendency for more overshoot and ringing. This is due to the resonance frequency being reduced with temperature, which results in a somewhat less damped modulation response (Figs. 4 and 5).

With the larger size multimode D1-VCSEL, we could transmit data error-free (BER $< 10^{-12}$) up to 40 Gbps at 25 °C and 35 Gbps at 85 °C. With the strongly single-mode D2-VCSEL, we could transmit data up to

bit-rates as high as 50 Gbps at 25 °C and 40 Gbps at 85 °C. These are the highest data rates reported for 1060 nm VCSELs. The D2 single-mode VCSEL is also energy efficient, with energy dissipation of only 100 fJ/bit at 50 Gbps and only 2.5 mA of bias current, which is on par with state-of-the-art at 850 nm [38]. At this low energy dissipation, the power consumption of the interconnect will be dominated by the power consumption of the electronics [9].

4. Long-reach VCSEL-MMF links

4.1. 1060 nm optimized multimode fiber

For the transmission experiments, we used a prototype MMF fabricated at Corning. The graded-index fiber has a 50 μm diameter core with an alpha-value of ~2.06 to minimize the differential mode delay and maximize the modal bandwidth at 1060 nm. The modal bandwidth, measured using an encircled flux launch [39], is > 5 GHz·km at this wavelength. Chromatic dispersion and attenuation are about –33 ps/nm/km and 0.95 dB/km, respectively.

4.2. Data transmission

In the first preliminary transmission experiment, we used the single-mode VCSEL, which reduces the impact of chromatic dispersion by its narrow spectral width and the impact of modal dispersion by mode-selective launch. To launch into the lowest order mode group of the fiber, the VCSEL near-field was projected on the center of the fiber end-face using an anti-reflection coated lens system with a magnification to produce an illumination spot with a size similar to the size of the fundamental mode of the MMF. The fiber was also held at a slight angle to eliminate optical feedback to the VCSEL. No optical isolator was used. Otherwise, the equipment was the same as used for the back-to-back large-signal modulation experiments (Section 3.3).

Fig. 8 shows the results from binary NRZ (OOK) transmission over 1000 m of MMF without equalization or FEC. The VCSEL was biased at 4 mA and we used both PRBS-7 and PRBS-15 to investigate penalties associated with the pattern length. The highest data rate is 25 Gbps where error-free transmission is achieved with −4 dBm of average power (PRBS-15). A penalty of 1.5 dB was observed when increasing the pattern length from PRBS-7 to PRBS-15. Measurements were also performed with PRBS-31, with no further penalty observed. We expect significantly higher data rates and/or longer transmission distances with equalization, FEC, and/or multilevel modulation.

Finally, a preliminary investigation of the impact of VCSEL-to-MMF misalignment has indicated an approximate ± 5 μm tolerance to achieve 25 Gbps error-free transmission over 1000 m MMF. The results from a more extensive investigation will be presented elsewhere.

5. Summary and outlook

We have demonstrated a new generation of high-speed oxide-confined 1060 nm single and multimode VCSELs for extended reach VCSEL-MMF optical interconnects. Two different designs were presented, where one promotes single-mode emission with a relatively large oxide aperture through weak transverse optical guiding and strong transverse confinement of optical gain. A single-mode VCSEL from this design was shown to support data rates up to 50 Gbps while a multimode VCSEL from the other design supports data rates up to 40 Gbps. Using mode-selective launch, we demonstrated error-free 25 Gbps transmission over 1000 m of 1060 nm optimized MMF with the single-mode VCSEL.

Further work, aiming at increasing both the data rate and the transmission distance, involves not only the development of VCSEL designs for higher modulation bandwidth but also investigations of the impact of launch conditions with both single and multimode VCSELs. The associated alignment tolerances should be quantified. Higher-order modulation formats, pre-emphasis, pulse shaping, equalization, FEC, etc. are also techniques that should be implemented to reach high data rates (e.g. 50 Gbps) over 2 km MMF as needed in mega-data centers [40].

Acknowledgements

The work at Chalmers is financially supported by the Hewlett Packard Enterprise Innovation Research Program and by the Swedish Foundation for Strategic Research. IQE Europe provided the epitaxial material for VCSEL fabrication.

References

[1] J.A. Tatum, D. Gazula, L.A. Graham, J.K. Guenter, R.H. Johnson, J. King, C. Kocot, G.D. Landry, I. Lyubomirsky, A.N. MacInnes, E.M. Shaw, K. Balemarthy, R. Shubochkin, D. Vaidya, M. Yan, F. Tang, VCSEL-based interconnects for current and future data centers, IEEE J. Lightwave Technol. 33 (2015) 727–732.
[2] D. Mahgerefteh, C. Thompson, C. Cole, G. Denoyer, T. Nguyen, I. Lyubomirsky, C. Kocot, J. Tatum, Techno-economic comparison of silicon photonics and multimode VCSELs, IEEE J. Lightwave Technol. 34 (2016) 233–242.
[3] M.J. Li, Novel optical fibers for data center applications, Proc. SPIE 9772 (2016) 977205-1-7.
[4] J.M. Castro, R. Pimpinella, B. Kose, P. Huang, B. Lanne, K. Szczerba, P. Westbergh, T. Lengyel, J.S. Gustavsson, A. Larsson, P.A. Andrekson, Investigation of 60 Gb/s 4-PAM using an 850 nm VCSEL and multimode fiber, IEEE J. Lightwave Technol. 34 (2016) 3825–3836.
[5] R. Safaisini, E. Haglund, P. Westbergh, J.S. Gustavsson, A. Larsson, 20 Gbit/s data transmission over 2 km multimode fiber using 850 nm mode filter VCSEL, Electron. Lett. 50 (2014) 40–42.
[6] G. Stepniak, A. Lewandowski, J.R. Kropp, N.N. Ledentsov, V.A. Shchukin, N. Ledentsov Jr., G. Schaefer, M. Agustin, J.P. Turiewicz, 54 Gbit/s OOK transmission using single-mode VCSEL up to 2.2 km MMF, Electron. Lett. 52 (2016) 633–635.
[7] I.C. Lu, C.C. Wei, H.Y. Chen, K.Z. Chen, C.H. Huang, K.L. Chi, J.W. Shi, F.I. Lai, D.H. Hsieh, H.C. Huo, W. Lin, S.W. Chiu, J. Chen, Very high bit-rate distance product using high-power single-mode 850 nm VCSEL with discrete multitone modulation formats through OM4 multimode fiber, IEEE J. Sel. Top. Quantum Electron. 21 (2015) 1701009.
[8] C. Kottke, C. Caspar, V. Jungnickel, R. Freund, M. Agustin, N.N. Ledentsov, High speed 160 Gb/s DMT VCSEL transmission using pre-equalization, in: Proc. Optical Fiber Communications Conference (2017) W4I.7.
[9] D.M. Kuchta, A.V. Rylyakov, C.L. Schow, J.E. Proesel, C. Baks, P. Westbergh, J.S. Gustavsson, A. Larsson, 64 Gb/s transmission over 57 m MMF using an NRZ modulated 850 nm VCSEL, in: Proc. Optical Fiber Communications Conference (2014) Th3C.2.
[10] J.J. Liu, K.L. Chi, C.C. Wei, T.C. Lin, C.Y. Chuang, X.N. Chen, J.W. Shi, J. Chen, High bit-rate distance product of 128 Gbps·km 4-PAM transmission over 2 km OM4 fiber using an 850 nm VCSEL and Volterra nonlinear equalizer, Proc. Optical Fiber Communications Conference (2017) W3G.5.
[11] T. Zuo, L. Zhang, J. Zhou, Q. Zhang, E. Zhou, G.N. Liu, Single lane 150 Gb/s, 100 Gb/s nd 70 Gb/s 4-PAM transmission over 100 m, 300 m and 500 m MMF using 25-G class 850 nm VCSEL, in: Proc. European Conference on Optical Communication (2016) 974-976.
[12] F. Chang, Y. Sun, R. Lingle, Y. Zhang, P. Cai, M. Huang, D. Pan, T. Gray, S. Bhoja, S. Nelson, J. Tatum, First demonstration of PAM4 transmission for record reach and high-capacity SWDM links over MMF using 40G/100G PAM4 IC chipset with real-time DSP, in: Proc. Optical Fiber Communications Conference (2017) Tu2B.2.
[13] J. Lavrencik, S. Varughese, V.A. Thomas, G. Landry, Y. Sun, R. Shubochkin, K. Balemarthy, J. Tatum, S.E. Ralph, 4λ x 100 Gbps VCSEL PAM-4 transmission over 105 m of wideband multimode fiber, in: Proc. Optical Fiber Communications Conference (2017) Tu2B.6.
[14] T.N. Huynh, F. Doany, D.M. Kuchta, D. Gazula, E. Shaw, J. O'Daniel, J. Tatum, 4x50 Gb/s NRZ short-wavelength division multiplexing VCSEL link over 50 m multimode fiber, in: Proc. Optical Fiber Communications Conference (2017) Tu2B.5.
[15] H. Hatakeyama, T. Anan, T. Akagawa, K. Fukatsu, N. Suzuki, K. Tokutome, M. Tsuji, Highly reliable high-speed 1.1 μm range VCSELs with InGaAs/GaAsP MQW, IEEE J. Quantum Electron. 46 (2010) 890–897.
[16] N. Suzuki, H. Hatakeyama, K. Fukatsu, T. Anan, K. Yashiki, M. Tsuji, 25 Gbit/s operation of InGaAs-based VCSELs, Electron. Lett. 42 (2006) 975–976.
[17] K. Yashiki, N. Suzuki, K. Fukatsu, T. Anan, H. Hatakeyama, M. Tsuji, 1.1 μm-range high-speed tunnel-junction vertical-cavity surface-emitting lasers, IEEE Photon. Techn. Lett. 19 (2007) 1883–1885.
[18] N. Suzuki, T. Anan, H. Hatakeyama, K. Fukatsu, K. Yashiki, K. Tokutome, T. Akagawa, M. Tsuji, High-speed 1.1 μm-range InGaAs-based VCSELs, IEICE Trans. Electron. E92-C (2009) 942–950.
[19] Y. Zheng, C.H. Lin, A.V. Barve, L.A. Coldren, p-type δ-doping of highly strained VCSELs for 25 Gbps operation, in: Proc. IEEE Photonics Conference (2012) 131-132.
[20] A. Tatarczak, Y. Zheng, G.A. Rodes, J. Estaran, C.H. Lin, A.V. Barve, R. Honoré, N. Larsen, L.A. Coldren, I.T. Monroy, 30 Gbps bottom-emitting 1060 nm VCSEL, in: Proc. European Conference on Optical Communication (2014), P.2.3.

[21] T. Suzuki, M. Funabashi, H. Shimizu, K. Nagashima, S. Kamiya, A. Kasukawa, 1060 nm 28 Gbps VCSEL development at Furukawa, Proc. SPIE 9001 (2014) 900104-1-9.
[22] J.B. Heroux, T. Kise, M. Funabashi, T. Aoki, C.L. Schow, A.V. Rylyakov, S. Nakagawa, Energy efficiency 1060 nm optical link operating up to 28 Gb/s, IEEE J. Lightwave Technol. 33 (2015) 733–740.
[23] T. Kise, T. Suzuki, M. Funabashi, K. Nagashima, H. Nasu, The development of the 1060 nm 28 Gb/s VCSEL and the characteristics of the multimode fiber link, Furukawa Rev. 46 (2015) 7–12.
[24] K. Nagashima, T. Kise, Y. Ishihawa, H. Nasu, A record 1 km MMF 25.78 Gb, s error-free link using a, 1060 nm DIC VCSEL, IEEE Photon. Techn. Lett. 28 (2015) 418–420.
[25] S.K. Pavan, J. Lavrenick, R. Shubochkin, Y. Sun, J. Kim, D. Vaidya, R. Lingle Jr., T. Kise, S. Ralph, 50 Gbit/s PAM-4 MMF transmission using 1060 nm VCSELs with reach beyond 200 m, in: Proc. Optical Fiber Communication Conference (2014) W1F.5.
[26] M. Tan, P. Rosenberg, W. Sorin, S. Mathai, G. Panotopoulos, G. Rankin, J. Straznicky, Progress towards low cost Tbps optical engines, in: Proc. IEEE Components, Packaging, and Manufacturing Technology Symposium (2015) 9–11.
[27] M. Tan, P. Rosenberg, W. Sorin, S. Mathai, G. Panotopoulos, G. Rankin, Universal photonic interconnect for data centers, in: Proc. Optical Fiber Communications Conference (2017) Tu2B.4.
[28] R. Rosales, M. Zorn, J.A. Lott, 30 GHz bandwidth with directly current-modulated 980 nm oxide-aperture VCSELs, IEEE Photon. Techn. Lett. (2017) pre-print available on-line.
[29] G. Larisch, P. Moser, J.A. Lott, D. Bimberg, Large bandwidth, small current density, and temperature stable 980 nm VCSELs, IEEE J. Quantum Electron. 53 (2017) 2400908.
[30] P. Westbergh, R. Safaisini, E. Haglund, J.S. Gustavsson, A. Larsson, M. Green, R. Lawrence, A. Joel, High-speed oxide-confined 850 nm VCSELs operating at 40 Gb/s up to 85°C, IEEE Photon. Techn. Lett. 25 (2013) 768–771.
[31] E. Haglund, P. Westbergh, J.S. Gustavsson, E.P. Haglund, A. Larsson, High-speed VCSELs with strong confinement of optical fields and carriers, IEEE J. Lightwave Technol. 34 (2016) 269–277.
[32] E.R. Hegblom, Engineering Oxide Apertures in Vertical-cavity Lasers, PhD thesis University of California Santa Barbara, 1999.
[33] E.R. Hegblom, B.J. Thibeault, R.L. Naone, L. Coldren, Vertical cavity lasers with tapered oxide apertures for low scattering loss, Electron. Lett. 33 (1997) 869–871.
[34] G.R. Hadley, Effective index model for vertical-cavity surface-emitting lasers, Opt. Lett. 20 (1995) 1483–1485.
[35] M. Balkanski, R.F. Wallis, Semiconductor Physics and Applications, chapter 10.3.1 Oxford University Press, Oxford, 2000.
[36] P. Westbergh, J.S. Gustavsson, B. Kögel, Å. Haglund, A. Larsson, Impact of photon lifetime on high-speed VCSEL dynamics, IEEE J. Sel. Top. Quantum Electron. 17 (2011) 1603–1613.
[37] E.P. Haglund, P. Westbergh, J.S. Gustavsson, A. Larsson, Impact of damping on high-speed large-signal VCSEL dynamics, IEEE J. Lightwave Technol. 33 (2015) 795–801.
[38] E. Haglund, P. Westbergh, J.S. Gustavsson, E.P. Haglund, A. Larsson, M. Geen, A. Joel, 30 GHz bandwidth 850 nm VCSEL with sub-fJ/bit energy dissipation at 25–50 Gbit/s, Electron. Lett. 51 (2015) 1096–1098.
[39] X. Chen, S.R. Bickham, J.E. Hurley, H.F. Liu, O.I. Dosunmu, M.J. Li, 300 m transmission over multimode fiber at 25 Fb/s using a multimode launch at 1310 nm, Opt. Exp. 21 (2013) 28968–28973.
[40] C. DeCusatis, Optical interconnect networks for data communications, IEEE J. Lightwave Technol. 32 (2014) 544–552.